Shear Stress Magnitude and Duration Modulates Matrix Composition and Tensile Mechanical Properties in Engineered Cartilaginous Tissue

Christopher V. Gemmiti[1] and **Robert E. Guldberg**[2]

[1]Coulter Department of Biomedical Engineering, Georgia Institute of Technology and Emory School of Medicine, Atlanta, GA

[2]Woodruff School of Mechanical Engineering, Georgia Institute of Technology, Atlanta, GA

Abstract

Cartilage tissue-engineering strategies aim to produce a functional extracellular matrix similar to that of the native tissue. However, none of the myriad approaches taken have successfully generated a construct possessing the structure, composition, and mechanical properties of healthy articular cartilage. One possible approach to modulating the matrix composition and mechanical properties of engineered tissues is through the use of bioreactor-driven mechanical stimulation. In this study, we hypothesized that exposing scaffold-free cartilaginous tissue constructs to seven days of continuous shear stress at 0.001-Pa or 0.1-Pa would increase collagen deposition and tensile mechanical properties compared to that of static controls. Histologically, type II collagen staining was evident in all construct groups, while a surface layer of type I collagen increased in thickness with increasing shear stress magnitude. The areal fraction of type I collagen was higher in the 0.1-Pa group (25.2±2.2%) than either the 0.001-Pa (13.6±3.8%) or the static (7.9%±1.5%) groups. Type II collagen content, as assessed by ELISA, was also higher in the 0.1-Pa group (7.5±2.1%) compared to the 0.001-Pa (3.0±2.25%) or static groups (3.7±3.2%). Temporal gene expression analysis showed a flow-induced increase in type I and II collagen expression within 24 hours of exposure. Interestingly, while the 0.1-Pa group showed higher collagen content, this group retained less sulfated glycosaminoglycans in the matrix over time in bioreactor culture. Increases in both tensile Young's modulus and ultimate strength were observed with increasing shear stress, yielding constructs possessing a modulus of nearly 5-MPa and strength of 1.3-MPa. This study demonstrates that shear stress is a potent modulator of both the amount and type of synthesized extracellular matrix constituents in engineered cartilaginous tissue with corresponding effects on mechanical function.

Keywords

bioreactor; tissue engineering; cartilage; type II collagen; mechanical properties

Introduction

Adult articular cartilage has little capacity for self repair and therefore typically requires intervention for restoration of function when damaged (Guilak *et al.* 2001; Poole 2003). If left untreated, both chondral and osteochondral defects typically progress to debilitating osteoarthritis (Brittberg *et al.* 1994). When considering the full spectrum of tissue damage,

Correspondence: Robert E. Guldberg, Ph.D. Georgia Institute of Technology, Institute for Bioengineering and Bioscience, 315 Ferst Drive, Atlanta, Georgia, U.S.A. 30332, Tel: 404-894-6589, Fax: 404-385-1397, robert.guldberg@me.gatech.edu.

indications at the far ends of the spectrum currently have treatments with acceptable outcomes: small, superficial asymptomatic lesions are remedied with arthroscopy, while advanced, full-thickness erosion is solved with total joint arthroplasty (Hunziker 2002). However, treatment options for patients in the middle of the spectrum who have defects of approximately 1-2 cm^2 are limited, often producing inferior tissues (Bae *et al.* 2006).

Efforts to engineer a tissue with properties similar to native tissue have explored many variables, including cell source (*e.g.*, species (Grogan *et al.* 2003; Raimondi *et al.* 2002) and/or anatomical location (Waldman *et al.* 2003a)), cell/tissue maturity (Obradovic *et al.* 2001), construct geometry (*e.g.*, scaffold (Freed *et al.* 1993; Gooch *et al.* 2001; Raimondi *et al.* 2002; Saini and Wick 2003) or scaffold-free (Adkisson *et al.* 2001; Fedewa *et al.* 1998; Jakob *et al.* 2001; Kandel *et al.* 1997; Mainil-Varlet *et al.* 2001)), growth factor supplementation (Blunk *et al.* 2002), and culture configuration (*e.g.*, bioreactor-driven mechanical stimulation (Freed *et al.* 1999; Hung *et al.* 2004; Martin *et al.* 2000; Mauck *et al.* 2000; Pazzano *et al.* 2000; Pei *et al.* 2002; Vunjak-Novakovic *et al.* 1999; Waldman *et al.* 2003b; Waldman *et al.* 2003c; Williams *et al.* 2002)). Many of these approaches have successfully created tissues with glycosaminoglycan content similar to that of native tissue. However, none have resulted in a tissue-engineered construct that possesses the proper organization and amount of type II collagen, the major structural protein in articular cartilage (Carver and Heath 1999; Freed *et al.* 1998; Hung *et al.* 2004; Waldman *et al.* 2003c).

Type II collagen's importance to the function of articular cartilage cannot be understated; in fact, its presence distinguishes articular (hyaline) cartilage from other cartilage types (*e.g.*, fibrous, elastic) (Poole *et al.* 2001) and is the most abundant protein in the matrix accounting for between 50-73% of the tissue's dry weight (LeBaron and Athanasiou 2000) and 80-85% of the total collagen (Cremer *et al.* 1998). This protein is known to play a crucial role in determining the tensile, shear and swelling properties of articular cartilage (Mow and Ratcliffe 1997). However, it is not merely the presence of type II collagen, but its complex interactions with the other matrix constituents (Poole 2003) such as type IX collagen, type XI collagen (Cremer *et al.* 1998) and cartilage oligomeric matrix protein (COMP) (Thur *et al.* 2001) which contributes to the function of articular cartilage. These interactions and the zonal distribution of type II collagen are paramount to the mechanical properties and thus the overall function of articular cartilage (Mow and Ratcliffe 1997).

While replicating the amount and organization of type II collagen remains a challenge, one promising approach to modulating the matrix composition and mechanical properties of engineering tissues is through the use of bioreactor-driven mechanical stimulation. It is thought that subjecting an *in vitro* developing tissue to mechanical signals (*e.g.*, compression, shear stress) similar to that witnessed by the *in vivo* native tissue may aid in coaxing the cells and tissue to respond accordingly. Since type II collagen is known to resist shear and tensile forces (Mow and Ratcliffe 1997), we hypothesized that imparting a shear stress to an engineered construct would result in the increased deposition of this protein. In previous studies, we developed a novel dual-chamber flow bioreactor to impart fluid-induced shear stress to a scaffold-free cartilaginous tissue of primary bovine chondrocytes origin (Gemmiti and Guldberg 2006). We found increases in type II collagen, total collagen and tensile mechanical properties of the shear-exposed cartilaginous tissue after only three days of flow. However, the collagen content and mechanical properties were still significantly less than that of native tissue, prompting further exploration of the parameter space.

In the experiments presented here, we hypothesized that cartilaginous tissue exposed to increased magnitudes of shear stress would translate to increased collagen deposition and

tensile mechanical properties. Lastly, we analyzed the gene expression over multiple time points in order to better understand the development and response of the tissue to fluid-induced shear stress.

Materials and Methods

Bioreactor

A custom-designed parallel-plate bioreactor was used for culturing and applying a consistent level of fluid-induced shear stress to the engineered tissues. Details of the bioreactor construction and underlying fluid mechanics have previously been described (Gemmiti and Guldberg 2006). Briefly, the bioreactor possesses two rectangular chambers (upper and lower) which are bisected by a semi-permeable (0.2-μm diameter pores, ~9% open area, nominally 10-μm thick) polycarbonate membrane (GE Osmonics, Minnetonka, MN), upon which the engineered tissue is grown (Figure 1).

Both chambers are loaded with nutrient media so that the cells residing in the tissue can feed from either side of the construct. Two culture configurations exist for the bioreactor: static and flow. In the static configuration, the upper chamber is allowed to exchange gases with the incubator via a non-sealing cover, which has an overhanging lip that discourages contaminants. In the flow configuration, a cap is affixed to the bioreactor in order to create a flow chamber of set length (L, 4.57 cm), width (b, 1.27 cm) and height (h, 350 μm) for a culture area of 5.8 cm^2. The height is altered by adding shims under the cap (outside the fluid flow path). A peristaltic pump recirculates nutrient media through the bioreactor via pump tubing and associated fittings at a constant volumetric flow rate (Q). As media flows through the flow chamber, a shear stress (τ_w) is applied to the top surface of the engineered tissue, and can be estimated using the following equation:

$$\tau_w = \frac{6\mu Q}{bh^2}$$

where τ_w is in Pa, μ is the media viscosity in Pa-sec, Q is the flow rate in mL/sec, b is the flow chamber width in cm and h is the fluid gap height in cm. This wall shear stress is estimated to be valid over more than 95% of the bioreactor length (Gemmiti and Guldberg 2006).

Cell Isolation and Seeding

Primary bovine articular chondrocytes were harvested from 2-4 week old calves (Research 87, Boylston, MA), as previously described (Gemmiti and Guldberg 2006). Briefly, harvest tissues were minced, incubated for 48 hours in 0.2% type II collagenase (Worthington Biochemical, Lakewood, NJ) in DMEM (Invitrogen, Carlsbad, CA), washed twice in DMEM containing 10% FBS (Hyclone, Logan, UT), pelleted and frozen in liquid nitrogen until time of seeding. Cells were thawed and counted using a haemocytometer, with viability assessed using trypan blue (Invitrogen). Cells were suspended at a concentration of 2.5×10^6 cells/mL in DMEM containing 10% FBS, 50-μg/mL ascorbic acid-2-phosphate (Sigma, St. Louis, MO), 10-mM non-essential amino acids (Invitrogen) and 10-mg/mL gentamycin (Invitrogen). 10×10^6 cells (in 4-mL media) were loaded into each bioreactor in the static configuration. 24 hours prior to the addition of cells, bioreactors were loaded with media in order to let serum proteins adsorb to the membrane and encourage cell adhesion. Media was exchanged every 48 hours throughout the experiment. The data presented in this manuscript represents a collection of three experiments, each using cells from a different donor.

Flow Experiments

All bioreactors remained in the static configuration for two weeks as cells secreted matrix and self-assembled a neo-tissue. After this pre-culture period, bioreactors were converted to the flow configuration and tissues were subjected to one of two estimated shear stress levels: 0.001-Pa (0.1-mL/min) and 0.1-Pa (3.0-mL/min). The additional 0.001-Pa group was added for two reasons: first, to examine any dose-dependent effect of shear on construct development, and second, to account for the media volume differences between the flowed (9-mL) and static (6-mL) groups. A third group of bioreactors was kept in the static configuration to remain as controls. In order to keep shear stress and flow rate constant, the upper flow surface (cap) was raised in 50-μm increments by adding additional shims during each feed (every 48 hours) to account for tissue growth, thereby keeping the flow chamber height (h) constant. Static bioreactors were fed 4-mL media in the upper chamber and approximately 2-mL in the bottom chamber. Flow bioreactors received approximately 7-mL in the flow loop and 2-mL in the bottom chamber. The increase in media volume was due to the additional ports and tubing in the flow configuration and was kept as close to the static condition as possible. With media exchanges every 48 hours, flow bioreactor tissues were therefore fed fresh media at a rate of approximately 1-mL per 2.2×10^6 cells per day, which is similar to other successful systems (Freed et al. 1998; Mauck et al. 2003; Pazzano et al. 2000; Vunjak-Novakovic et al. 1999). Feed volume rates lower than approximately 1-mL per 3.5×10^6 cells per day show significant hindrance of matrix maturation (Mauck et al. 2002); therefore we believe that this feed volume rate is sufficient to maintain viability of cells and transport of nutrients. Tissues remained in either the static or flow configuration for a period of one week.

At the end of the week, all tissues were removed from the bioreactors and divided up for various biochemical assays and mechanical tests. Prior to division, each tissue was weighed wet and had approximately 2-mm of the perimeter trimmed and discarded in order to minimize edge-effects. Tissue samples for all biochemical assays were frozen at -20°C, except for sections reserved for RNA isolation, which were flash-frozen in liquid nitrogen and stored at -80°C. Mechanical testing was performed immediately (details to follow).

In a separate series of experiments, tissues were harvested at time intervals of 2 hours, 24 hours, 3 days and 7 days specifically for gene expression analysis. These tissues were similarly trimmed, and the entire tissue was frozen immediately in liquid nitrogen and stored at -80°C.

Histology

For each bioreactor, a separate section of tissue was fixed for 24 hours in 10% neutral buffered formalin as well as 1% acid alcohol (1% glacial acetic acid in 95% reagent alcohol). Additionally, a section of native bovine articular cartilage and ligament was taken during harvest and subjected to the same fixation, processing and embedding to serve as a positive and negative tissue control (respectively) for each stain. After fixation, tissues were rinsed in PBS for 2 hours and stored at 4°C in 70% reagent alcohol until time of tissue processing and paraffin embedding. 5 μm sections were cut and mounted on slides: the acid alcohol-fixed sections were dedicated to immunohistochemistry and the formalin-fixed sections to basic histology stains. Each specimen was stained for the presence of specific proteins using antibodies against type I collagen (mouse monoclonal MAB3391, Chemicon Inc, Temecula, CA), type II and type IX collagen (mouse polyclonals II-II6B3 and B3-1 respectively, Developmental Hybridoma Studies Bank, Iowa City, IA), with a biotinylated anti-mouse secondary antibody (BA 2001, Vector Laboratories, Burlingame, CA), as well as type X collagen (rabbit polyclonal, kindly donated by Dr. Gary Gibson, Henry Ford Hospital, Detroit, MI) with a biotinylated goat anti-rabbit IgG (BA-1000, Vector) in

conjunction with the Vecastain ABC alkaline phosphatase kit (SK 5100 and AK 5000, Vector). Antigen retrieval was achieved with a 10 minute (60 minutes for type X collagen) digestion using Digest-All 3 (Invitrogen) at 37°C. For each staining session, a secondary-antibody control was included to ensure specificity of the stain.

Basic histological stains included routine hematoxylin and eosin (H&E) for gross morphology, 0.1% safranin-O with 0.02% fast green counterstain for the presence of sulfated glycosaminoglycans, and 0.1% picrosirius red for collagen presence and fiber alignment. As before, native bovine articular cartilage and tendon samples were run alongside experimental samples to verify proper staining.

Type I collagen presence was quantified using Image Pro software (MediaCybernetics, Inc., Silver Spring, MD) by selecting area stained red by the Vectastain alkaline phosphatase kit. Images at 10× magnification were taken sequentially along the entire length of the tissue (approximately five images per tissue) and analyzed: an area of interest was manually drawn around the entire tissue, then the software automatically calculated the number of pixels stained red (*i.e.*, type I collagen present) and the total number of pixels in the tissue. Data are expressed as "percent area stained" defined as the number of pixels representing type I collagen divided by the total number of pixels present in the tissue. Type II collagen or safranin-O were not quantified as all tissues were stained throughout.

Mechanical Testing

Fresh specimens were stamped into the shape of a dogbone (gauge length and width of 20-mm and 5-mm, respectively), loaded into soft-tissue grips of the ELF 3200 mechanical testing system (EnduraTEC / Bose, Eden Prairie, MN), and pulled to failure at a rate of 0.02-mm/sec. Force was recorded using a 5.6-lb load cell (Interface, Scotsdale, AZ) and displacement recorded via computer acquisition interface (WinTest, EnduraTEC). Stress and strain were calculated from the force and displacement data by adjusting for the tissue's cross-sectional area and gauge length respectively. From the stress-strain plot, the Young's modulus (linear portion of the curve) and ultimate stress (maximum stress obtained prior to failure) were calculated.

Matrix Composition Assays

For each bioreactor, two sections of approximately 50-mg of wet tissue were weighed, dried overnight (SpeedVac), and then weighed dry in order to calculate the water content. One tissue section was dedicated to proteinase-K digestion for sulfated gylcosaminoglycan (sGAG, sGAG in Tissue), DNA and total collagen assays; the other to pepsin / elastase digestion for type II collagen (ELISA assay). Spent medium was also collected on days 2, 4 and 6 for sGAG assay (sGAG in Medium) and subject to the same processing and analysis which is described below.

Proteinase-K tissue was digested in a 60°C water bath for 18-24 hours using 125-µg of freshly-prepared proteinase K (Worthington) in 1-mL of 100-mM ammonium acetate. Total collagen was determined via hydroxyproline content (Woessner 1961), whereby 100-µL of digest is hydrolyzed in 2-mL 6N HCl at 110°C for 24 hours, re-suspended in 0.25M sodium phosphate buffer, reacted with chloramine T (Mallinckrodt Baker, Phillipsburg, NJ) and p-dimethylaminobenzaldehyde (Mallinckrodt Baker) and read on a PowerWave spectrophotometer (Bio-Tek, Winooski, VT) at an optical density of 557 nm. Experimental samples were compared to standards of known hydroxyproline content, then converted to total collagen by using a conversion of 10:1 hydroxyproline:collagen (Berg 1982; Brandt *et al.* 1998). Purified type II collagen (Southern Biotech, Birmingham, AL) was hydrolyzed using the previously described process to support use of this ratio. sGAG content was

quantified by reacting 50-fold diluted proteinase-K digest with dimethyl-methylene blue (Farndale *et al.* 1986; Farndale *et al.* 1982) (DMMB, Aldrich), read on the PowerWave spectrophotometer at 525-nm and compared to standards of chondroitin sulfate. DNA content was quantified by reacting samples with the Hoescht 33258 dye (Kim *et al.* 1988) (Sigma), read on PerkinElmer (Wellesley, MA) HTS 7000 fluorometric plate reader at excitation/emission wavelengths of 360/465 nm and compared to standards of calf thymus DNA in 1X TEN buffer.

Tissues for the capture enzyme-linked immunosorbent assay (ELISA, Chondrex Inc., Redmond, WA) were digested at 4°C in pepsin (P7012, Sigma) for 72 hours, followed by a 24 hour digest in pancreatic elastase (LS006365, Worthington Biochemical) in accordance with manufacturer's protocol. Digested samples were compared against type II collagen standards (supplied with kit) and read on the PowerWave spectrophotometer at an optical density of 490 nm.

RNA Isolation, Reverse Transcription and Quantitative PCR

Tissues dedicated for RNA isolation were flash frozen in liquid nitrogen and stored at -80°C. RNA was isolated using the TRIspin method (Reno *et al.* 1997) by first grinding the tissue to a fine powder under liberal amounts of liquid nitrogen, homogenized by suspending in TRIzol reagent (Invitrogen) and repeatedly passing through a 20-gauge needle. After a 15-min incubation in TRIzol at room temperature to dissociate nucleoprotein complexes and centrifugation, supernatant was combined with 0.2 mL chloroform. The upper, clear, aqueous phase was removed and mixed with 0.5-mL 100% isopropyl alcohol to precipitate the RNA in a new tube. After centrifugation, the remaining pellet was resuspended in 350-μL RLT buffer (RNeasy kit; QIAgen, Valencia, CA) plus 3.5-μL β-mercaptoethanol. This lysate was pipetted directly onto a QIAshredder column (QIAgen) and then combined with 350-μL 70% ethanol. This supernatant was added to an RNeasy column (QIAgen) and RNA was isolated according to manufacturer's protocol. Total RNA was quantified using the Nanodrop ND-1000 spectrophotometer (Nanodrop Technologies, Inc., Wilmington, DE); samples with a 260:280 (nm) absorbance ratio less than 2.00 were considered impure and not used in analysis (NanoDrop_Technologies 2005). cDNA was generated according to manufacturer's instructions (A3500 Reverse Transcription Kit; Promega, Madison, WI) using 1-μg RNA per sample. Samples were frozen at -20°C until time of qPCR.

Gene expression was quantified using SYBR Green intercalating dye (Applied Biosystems, Foster City, CA) and the Prism 7770 Sequence Detector (Applied Biosystems; 40 cycles: melting = 15 s at 95°C; annealing and extension = 60 s at 60°C). The cycle number where the measured fluorescence exceeds a threshold (cT) was calculated automatically using the Applied Biosystems software package. Experimental samples, standards and no-template controls were run in duplicate in 50-μL reaction volumes. Standards were generated from bovine chondrocyte cDNA amplicons using primers listed below (Table 1). For each well, 1-μL of cDNA was combined with nuclease-free water (23.75-μL), forward primer (0.125-μL), reverse primer (0.125-μL) and SYBR Green Master Mix (25-μL; Applied Biosystems). Melting curves (data not presented) were run at least once for each primer set and experimental condition to rule out false-positive signals generated by non-specific double-stranded DNA sequence amplification. Primers for each gene are listed below in Table I.

Data are expressed normalized by internal cellular housekeeping gene, glyceraldehyde-3-phosphate dehydrogenase (GAPDH).

Statistics

Samples from three experiments were pooled and analyzed using Minitab software (State College, PA) by ANOVA general linear model and pair-wise comparisons, with statistical significance assigned to $p \leq 0.05$. Data are expressed as average ± standard error of the mean. Sample size is 14 for each group, unless otherwise noted. As previously stated, the data presented here is a collection of three experiments. In each individual experiment, the sample size of each condition varied, with no less than N=3 in any condition. Statistical analysis was conducted on the aggregate of these experiments, N=14 per condition total, with additional analysis on cross-experimental variability. No effect of experiment was seen.

Results

Histology

After 7 days of continuous flow, constructs stained positively throughout for type II collagen and sulfated glycosaminoglycans (Figure 2). There appeared to be a thicker band of type I collagen in the 0.1-Pa group compared to the 0.001-Pa and static groups, yet this band was restricted to the top surface in all groups. Co-localized in this band of type I collagen was an increase in cell density, with most cells assuming a more flattened, fibroblastic morphology. This band appeared to have a concentration of oriented collagen fibers, as witnessed in the picrosirius red stains under birefringent light. The area of intense type I collagen staining corresponded with a lack of type IX presence and a decrease in intensity of safranin-O stain as well. While not shown, no tissue stained for type X collagen and all positive and negative controls showed expected antibody specificity.

Matrix Composition

There were no significant differences among groups in terms of tissue weight (~270-mg), water content (~87% water) or thickness (~310-μm), although constructs in the 0.1-Pa group contained significantly more cells (DNA) than the 0.001-Pa or static control groups (Figure 3A). Although higher in DNA content, the tissues exposed to 0.1-Pa possessed significantly less sGAG on both a per-cell (Figure 3B) and per-dry weight (Figure 3C) basis than the other groups. These data are corroborated by both the qualitative assessment of the safranin-O staining (Figure 2) as well as the significant increase in sGAG present in the media (Figure 3D). Not only was the amount of sGAG in the media significantly higher in the 0.1-Pa group at each time point, but the release increased with time. Interestingly, when the sGAG present in the tissues was added to that in the media, the total sGAG was not different among groups (data not shown).

In terms of collagen, 0.1-Pa shear exposed tissues had more total collagen on a per-dry weight basis than the other groups (Figure 4A). This was not the case on a per-cell basis (Figure 4B), where the static controls were significantly higher than either of the flowed tissues. According to the histomorphometric analysis, type I collagen was present in a significantly greater percentage area of the tissue in the 0.1-Pa group (25.2±2.2%) compared to either the 0.001-Pa (13.6±3.8%) or the static (7.9%±1.5%) groups (Figure 4C). There was no difference between 0.001-Pa and static groups. Type II collagen content, as assessed by ELISA (Figure 4D), was also higher in the 0.1-Pa group (7.5±2.1%) compared to the 0.001-Pa (3.0±2.25%) or static groups (3.7±3.2%).

Mechanical Testing

A dose-dependent increase in tensile Young's modulus and ultimate strength was observed with increasing shear stress (Figure 5). While both flow groups were significantly higher than the static, the 0.1-Pa group showed the greatest increase up to nearly 5-MPa in modulus and 1.3-MPa in strength.

Gene Expression

Expression of type I and type II collagen were modulated by the magnitude and duration of shear stress (Figure 6). No significant differences were observed for the expression of aggrecan (not shown). While GAPDH levels did vary across time points, no significant difference was typically found between groups at a given time point. One exception was between the static and 0.001-Pa group at Day 7 which were significantly different ($p<0.05$). This difference did not have an impact since no significant difference was found between the static and 0.001-Pa groups for either type I or type II collagen expression, whether normalized by GAPDH or total RNA.

Type II collagen expression in the 0.1-Pa group was significantly decreased relative to the 0.001-Pa and static groups initially at the 2-hour time point, but rebounded to a significantly increased level (relative to the same groups) at the 24-hour time point. No differences between groups were observed by 7 days. Type I collagen followed similar trends in that it was significantly up-regulated at 24-hours and 3-days compared to the other groups. At the 2-hour and 7-day time points, no difference was observed for the 0.1-Pa group compared to the others. These trends are consistent with the previously described quantitative protein data (total collagen, ELISA and histomorphometry) and immunohistochemical observations.

The magnitude of shear stress produced altered gene expression time course profiles for each gene. The 0.001-Pa group maintained relatively low gene expression levels over time for type I and II collagen (with the exception of the 2-hour time point) as opposed to the 0.1-Pa group which showed a more dynamic response.

Discussion

While many strategies aim to increase similarity of engineered cartilaginous tissue to that of native tissue, none have achieved this goal. In particular, the amount and organization (*e.g.*, fiber orientation, interplay with other matrix molecules) of type II collagen in engineered tissues is consistently inferior to that in native tissue (Carver and Heath 1999; Freed *et al.* 1998; Hung *et al.* 2004; Waldman *et al.* 2003c). This crucial protein has direct effects on the unique mechanical properties of articular cartilage (Mow and Ratcliffe 1997). Type II collagen is most responsible for trapping the proteoglycans in the fibrillar matrix (Buckwalter and Mankin 1998), determining the tensile mechanical properties and resisting shearing deformations (Mow and Ratcliffe 1997) and has further been shown to have a positive correlation with the compressive properties (Sah *et al.* 1996). Given type II collagen's essential role in cartilage function and its deficiency in tissue-engineered constructs, we tested the hypothesis that shear stress enhances the composition and mechanical properties of cartilaginous tissue grown in a novel flow bioreactor.

We recently developed a dual-chambered flow bioreactor and demonstrated that short-term flow-mediated shear stress increases type II collagen content and tensile mechanical properties after three days of flow (Gemmiti and Guldberg 2006). While these results were promising, the engineered tissue lacked a matrix composition or mechanical properties similar to that of native tissue. In order to expand and improve upon these results, we extended the duration of flow to seven days in the hopes of further increasing type II collagen content and mechanical properties in this study. Indeed, extending the duration of exposure to hydrodynamic shear stress further increased the total and type II collagen content compared to controls, but at the expense of an increase in type I collagen presence and decrease of sGAG in the tissue.

Other hydrodynamic bioreactors have been shown to modulate the response of chondrocytes using fluid-induced shear stress in both monolayer (Malaviya *et al.* 1998; Malaviya and

Nerem 2002; Smith *et al.* 1995) and tissue-engineered systems (Freed *et al.* 1999; Hung *et al.* 2004; Martin *et al.* 2000; Pazzano *et al.* 2000; Pei *et al.* 2002; Vunjak-Novakovic *et al.* 1999; Waldman *et al.* 2003b; Waldman *et al.* 2003c; Williams *et al.* 2002). One drawback of many hydrodynamic systems used in tissue engineering is the heterogeneous field of shear stress applied to the cells and tissues. This heterogeneity arises due to the turbulent flows generated by the bioreactor and tissue (*e.g.*, spinner flask (Sucosky *et al.* 2004; Vunjak-Novakovic *et al.* 1999)) or the perfusion of media through a complex three-dimensional geometry of a scaffold (Raimondi *et al.* 2002). To circumvent this problem, we apply shear stress using a parallel-plate bioreactor (founded on Poiseuille fluid mechanics (Fox and McDonald 1992)) in conjunction with a scaffold-free tissue. The parallel plate design created a shear stress magnitude estimated to be consistent over more than 95% of the bioreactor's length (Gemmiti and Guldberg 2006). The goal to improve the engineered cartilaginous tissue's similarity to native tissue prompted the exploration of extended durations and different magnitudes of shear stress.

After seven days of flow, type I collagen, type II collagen, total collagen were increased in the 0.1-Pa group compared to the other two groups. The 0.001-Pa group was not different from the static controls for any of these metrics. Thus, while the shear stress-mediated increase in type II collagen evident after three days of flow was indeed extended to seven days of flow, there was an emergence of type I collagen. While type I collagen was present in all tissues, it was significantly increased in the 0.1-Pa group where more than 25% of the tissue's total area was stained positively for type I collagen. The qPCR data corroborates this histological observation, as the 0.1-Pa group showed the highest expression of type I collagen at Days 1 and 3. Deposition of type I collagen was relegated only to the flow-exposed surface of the tissue along with flattened, fibroblast-like cells. The presence of type I collagen co-localized with cells of fibroblast morphology at the construct surface has been observed in other studies using dynamic fluid flow (Martin *et al.* 2000; Vunjak-Novakovic *et al.* 1999) and studies with long-term (67 days) culture (Seidel *et al.* 2004). Appearance of type I collagen is more reminiscent of fibrocartilage, which contains a mixture of type I and type II collagen. The mechanical properties of fibrocartilage are inferior compared to articular cartilage when cyclic load bearing capabilities are required (Minas and Nehrer 1997).

Another consequence of the extended duration of flow was the depletion of sGAG in the tissue and the concurrent increase in sGAG present in the media in the 0.1-Pa group compared to the other groups. It is unknown whether or not this sGAG in the media was extracted from the tissue or merely released (and not incorporated) by the cells. Others have found sGAG content to be sensitive to fluid-flow environment in a variety of bioreactors, including static flasks, mixed flasks (turbulent shear) and rotating vessels (laminar shear) (Vunjak-Novakovic *et al.* 1999). Furthermore, sGAG leaching into the media from engineered constructs has been shown to be affected by fluid flow magnitude (Gooch *et al.* 2001), suggesting that the increase in sGAG in the media was probably lost from the matrix and released from the cells. One way to better separate these possible mechanisms is to assay the media and histology at closer intervals (i.e., every 12 hours). Interestingly, the total amount of sGAG produced did not vary among groups, when the sGAG in the tissue was added to that found in the media.

Consistent with the increase in total collagen, the 0.1-Pa tissues exhibited a greater tensile modulus and ultimate strength compared to the other two groups. Despite not showing any significant increase in total collagen, type I or type II collagen, the 0.001-Pa group showed a significant but moderate increase in mechanical properties over static controls as well. This may be due to an increase in matrix organization, as picrosirius red staining showed a denser band of collagen fibers on the top surface. Even though the application of shear stress

increased the tensile mechanical properties, all groups were still significantly less than that of native tissue for both modulus (~12MPa) and ultimate strength (~5 MPa) (Williamson *et al.* 2003). Nonetheless, the modulus of 4.89±0.14 MPa attained by the 0.1-Pa group agrees well with that found by others using scaffold-free constructs after eight weeks of culture (4.8±0.1 MPa) (Fedewa *et al.* 1998).

The biochemical basis for the increase in mechanical properties is unknown, but can reasonably be attributed to the increase in collagen content. This conclusion is based on collagen's known role of bearing the tensile loads in the native matrix and our observed concurrent increases in collagen and mechanical properties in our system. Still to be determined is whether the increase in mechanical strength is more due to type I collagen, type II collagen, or an increase in matrix organization. The picrosirius red staining did show a compaction of stratified collagen with the application of flow, although this stain does not distinguish among collagen types. The degree of cross-linking within the collagen network, which also may have affected the mechanical properties, was not tested. Interestingly, these increases in mechanical properties come despite a decrease in sGAG retained in the matrix in the 0.1-Pa group. This is reminiscent of others' observations that collagen (compared to proteoglycans) is most responsible for determining the tensile mechanical properties (Mow and Ratcliffe 1997).

We can also reasonably conclude that the effects seen in this system were not due to an increase in flux through the tissue. Mathematical models of a porous medium (cartilage) subject to Poiseuille flow using bioreactor dimensions and parameters similar to ours suggest that there is very limited fluid flux through the tissue (Hou et al. 1989; Pierre et al. 2007). In fact, intra-tissue flux would only occur if the tissue permeability was approximately eight orders of magnitude higher. We independently calculated the permeability in several of our specimens based on empirical data (not shown), and confirmed that very little flux occurred through our tissue. While the shear effects visually appear to "penetrate" through the matrix (as evidenced by the thick type I collagen band), this was probably less due to penetration and more likely due to a surface-relegated affect which builds as the tissue thickness increases over time. Whether or not thicker constructs engineered in the same fashion will allow for greater flux through the construct is unknown. But given the increase in permeability required to allow for appreciable flux, thicker tissues will probably not be exposed to a flux different than these thin constructs.

Certainly, one limitation of the assessment of the mechanical properties was the lack of compressive data. Because of the thickness of these tissues (~310-μm), it was difficult to get reliable, repeatable data for the compressive properties. Future experiments will engineer thicker (~1 mm) constructs in the bioreactor system which may improve the outcome of the compressive testing. Another consequence of the thickness and lack of mechanical integrity is that tissues could not be precisely sectioned into horizontal sections (either fresh or frozen). If this was accomplished, localizing effects of shear for biochemical or biomechanical properties would have been possible. It is our hope that thicker tissues will allow for this.

This study showed that shear stress magnitude and duration modulate the matrix composition and tensile mechanical properties of engineered cartilaginous tissue. While type II collagen and the tensile mechanical properties were increased with the highest level of shear stress, this came at the expense of an increase in type I collagen presence and depletion of sGAG from the matrix. Fluid induced shear stress is certainly a potent modulator of tissue development and requires greater understanding if it is to be employed to generate a functional articular cartilage construct. Intermittent or oscillatory flows may be necessary to preserve the pro-hyaline effects (increase in type II collagen, tensile mechanical

properties) but discourage the pro-fibrocartilaginous effects (type I collagen). Further exploration of the parameter space in the bioreactor will aid in attaining our goal of understanding the effects of fluid flow on engineered cartilaginous tissue.

Acknowledgments

References

Adkisson HD, Gillis MP, Davis EC, Maloney W, Hruska KA. In vitro generation of scaffold independent neocartilage. Clin Orthop. 2001; (391 Suppl):S280–94. [PubMed: 11603712]

Bae DK, Yoon KH, Song SJ. Cartilage healing after microfracture in osteoarthritic knees. Arthroscopy. 2006; 22(4):367–74. [PubMed: 16581448]

Berg, RA. Determination of 3 and 4 hydroxyproline. In: Frederiksen, LCaD, editor. Methods of Enzymology. New York: New York Academic Press; 1982. p. 393-394.

Blunk T, Sieminski AL, Gooch KJ, Courter DL, Hollander AP, Nahir AM, Langer R, Vunjak-Novakovic G, Freed LE. Differential effects of growth factors on tissue-engineered cartilage. Tissue Eng. 2002; 8(1):73–84. [PubMed: 11886656]

Brandt, KD.; Doherty, M.; Lohmander, LS. Osteoarthritis. New York: Oxford University Press; 1998. Composition and structure of articular cartilage; p. 110-111.

Brittberg M, Lindahl A, Nilsson A, Ohlsson C, Isaksson O, Peterson L. Treatment of deep cartilage defects in the knee with autologous chondrocyte transplantation. N Engl J Med. 1994; 331(14):889–95. [PubMed: 8078550]

Buckwalter JA, Mankin HJ. Articular cartilage: tissue design and chondrocyte-matrix interactions. Instr Course Lect. 1998; 47:477–86. [PubMed: 9571449]

Carver SE, Heath CA. Influence of intermittent pressure, fluid flow, and mixing on the regenerative properties of articular chondrocytes. Biotechnol Bioeng. 1999; 65(3):274–81. [PubMed: 10486125]

Cremer MA, Rosloniec EF, Kang AH. The cartilage collagens: a review of their structure, organization, and role in the pathogenesis of experimental arthritis in animals and in human rheumatic disease. J Mol Med. 1998; 76(3-4):275–88. [PubMed: 9535561]

Farndale RW, Buttle DJ, Barrett AJ. Improved quantitation and discrimination of sulphated glycosaminoglycans by use of dimethylmethylene blue. Biochim Biophys Acta. 1986; 883(2):173–7. [PubMed: 3091074]

Farndale RW, Sayers CA, Barrett AJ. A direct spectrophotometric microassay for sulfated glycosaminoglycans in cartilage cultures. Connect Tissue Res. 1982; 9(4):247–8. [PubMed: 6215207]

Fedewa MM, Oegema TR Jr, Schwartz MH, MacLeod A, Lewis JL. Chondrocytes in culture produce a mechanically functional tissue. J Orthop Res. 1998; 16(2):227–36. [PubMed: 9621897]

Fox, R.; McDonald, A. Introduction to Fluid Mechanics. New York: John Wiley & Sons, Inc.; 1992.

Freed LE, Hollander AP, Martin I, Barry JR, Langer R, Vunjak-Novakovic G. Chondrogenesis in a cell-polymer-bioreactor system. Exp Cell Res. 1998; 240(1):58–65. [PubMed: 9570921]

Freed LE, Martin I, Vunjak-Novakovic G. Frontiers in tissue engineering. In vitro modulation of chondrogenesis. Clin Orthop. 1999; (367 Suppl):S46–58. [PubMed: 10546635]

Freed LE, Vunjak-Novakovic G, Langer R. Cultivation of cell-polymer cartilage implants in bioreactors. J Cell Biochem. 1993; 51(3):257–64. [PubMed: 8501127]

Gemmiti CV, Guldberg RE. Fluid flow increases type II collagen deposition and tensile mechanical properties in bioreactor-grown tissue-engineered cartilage. Tissue Eng. 2006; 12(3):469–79. [PubMed: 16579680]

Gooch KJ, Kwon JH, Blunk T, Langer R, Freed LE, Vunjak-Novakovic G. Effects of mixing intensity on tissue-engineered cartilage. Biotechnol Bioeng. 2001; 72(4):402–7. [PubMed: 11180060]

Grogan SP, Rieser F, Winkelmann V, Berardi S, Mainil-Varlet P. A static, closed and scaffold-free bioreactor system that permits chondrogenesis in vitro. Osteoarthritis Cartilage. 2003; 11(6):403–11. [PubMed: 12801480]

Guilak F, Butler DL, Goldstein SA. Functional tissue engineering: the role of biomechanics in articular cartilage repair. Clin Orthop. 2001; (391 Suppl):S295–305. [PubMed: 11603713]

Hou JS, Holmes MH, Lai WM, Mow VC. Boundary conditions at the cartilage-synovial fluid interface for joint lubrication and theoretical verifications. J Biomech Eng. 1989; 111(1):78–87. [PubMed: 2747237]

Hung CT, Mauck RL, Wang CC, Lima EG, Ateshian GA. A paradigm for functional tissue engineering of articular cartilage via applied physiologic deformational loading. Ann Biomed Eng. 2004; 32(1):35–49. [PubMed: 14964720]

Hunziker EB. Articular cartilage repair: basic science and clinical progress. A review of the current status and prospects. Osteoarthritis Cartilage. 2002; 10(6):432–63. [PubMed: 12056848]

Jakob M, Demarteau O, Schafer D, Hintermann B, Dick W, Heberer M, Martin I. Specific growth factors during the expansion and redifferentiation of adult human articular chondrocytes enhance chondrogenesis and cartilaginous tissue formation in vitro. J Cell Biochem. 2001; 81(2):368–77. [PubMed: 11241676]

Kandel RA, Boyle J, Gibson G, Cruz T, Speagle M. In vitro formation of mineralized cartilagenous tissue by articular chondrocytes. In Vitro Cell Dev Biol Anim. 1997; 33(3):174–81. [PubMed: 9112125]

Kim YJ, Sah RL, Doong JY, Grodzinsky AJ. Fluorometric assay of DNA in cartilage explants using Hoechst 33258. Anal Biochem. 1988; 174(1):168–76. [PubMed: 2464289]

LeBaron RG, Athanasiou KA. Ex vivo synthesis of articular cartilage. Biomaterials. 2000; 21(24): 2575–87. [PubMed: 11071607]

Mainil-Varlet P, Rieser F, Grogan S, Mueller W, Saager C, Jakob RP. Articular cartilage repair using a tissue-engineered cartilage-like implant: an animal study. Osteoarthritis Cartilage. 2001; 9 A:S6–15. [PubMed: 11680690]

Malaviya, P.; Hunter, CJ.; Seliktar, D.; Schreiber, R.; Symons, KT.; Ratcliffe, A.; Nerem, RM. Fluid-induced shear stresses promote chondrocyte phenotypic alteration. Transactions of the Orthopaedic Research Society 44th Annual Meeting; 1998. p. 228

Malaviya P, Nerem RM. Fluid-induced shear stress stimulates chondrocyte proliferation partially mediated via TGF-beta1. Tissue Eng. 2002; 8(4):581–90. [PubMed: 12201998]

Martin I, Obradovic B, Treppo S, Grodzinsky AJ, Langer R, Freed LE, Vunjak-Novakovic G. Modulation of the mechanical properties of tissue engineered cartilage. Biorheology. 2000; 37(1-2):141–7. [PubMed: 10912186]

Mauck RL, Seyhan SL, Ateshian GA, Hung CT. Influence of seeding density and dynamic deformational loading on the developing structure/function relationships of chondrocyte-seeded agarose hydrogels. Ann Biomed Eng. 2002; 30(8):1046–56. [PubMed: 12449765]

Mauck RL, Soltz MA, Wang CC, Wong DD, Chao PH, Valhmu WB, Hung CT, Ateshian GA. Functional tissue engineering of articular cartilage through dynamic loading of chondrocyte-seeded agarose gels. J Biomech Eng. 2000; 122(3):252–60. [PubMed: 10923293]

Mauck RL, Wang CC, Oswald ES, Ateshian GA, Hung CT. The role of cell seeding density and nutrient supply for articular cartilage tissue engineering with deformational loading. Osteoarthritis Cartilage. 2003; 11(12):879–90. [PubMed: 14629964]

Minas T, Nehrer S. Current concepts in the treatment of articular cartilage defects. Orthopedics. 1997; 20(6):525–38. [PubMed: 9195635]

Mow, V.; Ratcliffe, A. Structure and Function of Articular Cartilage and Meniscus. In: Mow, V.; Hayes, W., editors. Basic Orthopaedic Biomechanics. 2. Philadelphia: Lippincott-Raven Publishers; 1997. p. 113-177.

NanoDrop_Technologies. ND-1000 Spectrophotometer v3.2 User's Manual. Wilmington: 2005.

Obradovic B, Martin I, Padera RF, Treppo S, Freed LE, Vunjak-Novakovic G. Integration of engineered cartilage. J Orthop Res. 2001; 19(6):1089–97. [PubMed: 11781010]

Pazzano D, Mercier KA, Moran JM, Fong SS, DiBiasio DD, Rulfs JX, Kohles SS, Bonassar LJ. Comparison of chondrogensis in static and perfused bioreactor culture. Biotechnol Prog. 2000; 16(5):893–6. [PubMed: 11027186]

Pei M, Solchaga LA, Seidel J, Zeng L, Vunjak-Novakovic G, Caplan AI, Freed LE. Bioreactors mediate the effectiveness of tissue engineering scaffolds. FASEB J. 2002; 16(12):1691–4. [PubMed: 12207008]

Pierre J, Gemmiti CV, Kolambkar YM, Oddou C, Guldberg RE. Theoretical analysis of engineered cartilage oxygenation: influence of construct thickness and media flow rate. Biomech Model Mechanobiol. 2007

Poole AR. What type of cartilage repair are we attempting to attain? J Bone Joint Surg Am. 2003; 85-A 2:40–4. [PubMed: 12721344]

Poole AR, Kojima T, Yasuda T, Mwale F, Kobayashi M, Laverty S. Composition and structure of articular cartilage: a template for tissue repair. Clin Orthop. 2001; 1(391 Suppl):S26–33. [PubMed: 11603710]

Raimondi MT, Boschetti F, Falcone L, Fiore GB, Remuzzi A, Marinoni E, Marazzi M, Pietrabissa R. Mechanobiology of engineered cartilage cultured under a quantified fluid-dynamic environment. Biomech Model Mechanobiol. 2002; 1(1):69–82. [PubMed: 14586708]

Reno C, Marchuk L, Sciore P, Frank CB, Hart DA. Rapid isolation of total RNA from small samples of hypocellular, dense connective tissues. Biotechniques. 1997; 22(6):1082–6. [PubMed: 9187757]

Sah RL, Trippel SB, Grodzinsky AJ. Differential effects of serum, insulin-like growth factor-I, and fibroblast growth factor-2 on the maintenance of cartilage physical properties during long-term culture. J Orthop Res. 1996; 14(1):44–52. [PubMed: 8618165]

Saini S, Wick TM. Concentric cylinder bioreactor for production of tissue engineered cartilage: effect of seeding density and hydrodynamic loading on construct development. Biotechnol Prog. 2003; 19(2):510–21. [PubMed: 12675595]

Seidel JO, Pei M, Gray ML, Langer R, Freed LE, Vunjak-Novakovic G. Long-term culture of tissue engineered cartilage in a perfused chamber with mechanical stimulation. Biorheology. 2004; 41(3-4):445–58. [PubMed: 15299276]

Smith RL, Donlon BS, Gupta MK, Mohtai M, Das P, Carter DR, Cooke J, Gibbons G, Hutchinson N, Schurman DJ. Effects of fluid-induced shear on articular chondrocyte morphology and metabolism in vitro. J Orthop Res. 1995; 13(6):824–31. [PubMed: 8544017]

Sucosky P, Osorio DF, Brown JB, Neitzel GP. Fluid mechanics of a spinner-flask bioreactor. Biotechnol Bioeng. 2004; 85(1):34–46. [PubMed: 14705010]

Thur J, Rosenberg K, Nitsche DP, Pihlajamaa T, Ala-Kokko L, Heinegard D, Paulsson M, Maurer P. Mutations in cartilage oligomeric matrix protein causing pseudoachondroplasia and multiple epiphyseal dysplasia affect binding of calcium and collagen I, II, and IX. J Biol Chem. 2001; 276(9):6083–92. [PubMed: 11084047]

Vunjak-Novakovic G, Martin I, Obradovic B, Treppo S, Grodzinsky AJ, Langer R, Freed LE. Bioreactor cultivation conditions modulate the composition and mechanical properties of tissue-engineered cartilage. J Orthop Res. 1999; 17(1):130–8. [PubMed: 10073657]

Waldman SD, Grynpas MD, Pilliar RM, Kandel RA. The use of specific chondrocyte populations to modulate the properties of tissue-engineered cartilage. J Orthop Res. 2003a; 21(1):132–8. [PubMed: 12507590]

Waldman SD, Spiteri CG, Grynpas MD, Pilliar RM, Hong J, Kandel RA. Effect of biomechanical conditioning on cartilaginous tissue formation in vitro. J Bone Joint Surg Am. 2003b; 85-A 2:101–5. [PubMed: 12721351]

Waldman SD, Spiteri CG, Grynpas MD, Pilliar RM, Kandel RA. Long-term intermittent shear deformation improves the quality of cartilaginous tissue formed in vitro. J Orthop Res. 2003c; 21(4):590–6. [PubMed: 12798056]

Williams KA, Saini S, Wick TM. Computational fluid dynamics modeling of steady-state momentum and mass transport in a bioreactor for cartilage tissue engineering. Biotechnol Prog. 2002; 18(5):951–63. [PubMed: 12363345]

Williamson AK, Chen AC, Masuda K, Thonar EJ, Sah RL. Tensile mechanical properties of bovine articular cartilage: variations with growth and relationships to collagen network components. J Orthop Res. 2003; 21(5):872–80. [PubMed: 12919876]

Woessner JF Jr. The determination of hydroxyproline in tissue and protein samples containing small proportions of this imino acid. Arch Biochem Biophys. 1961; 93:440–7. [PubMed: 13786180]
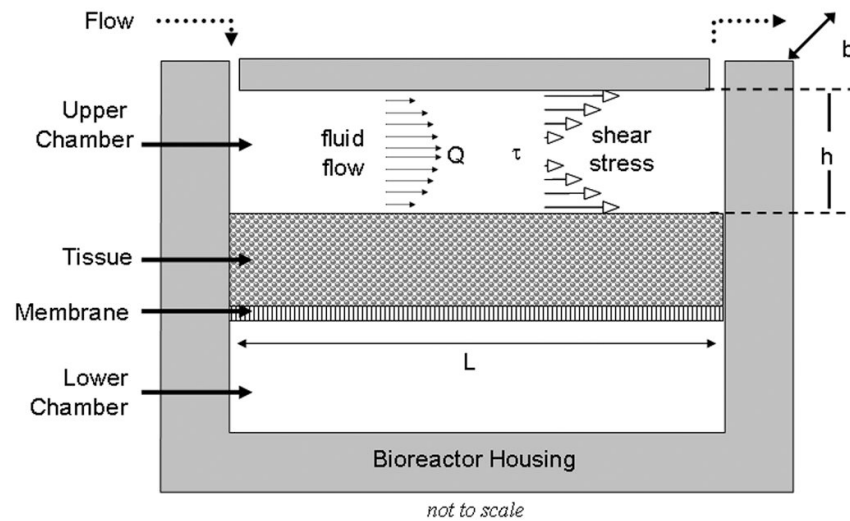
Figure 1.
Schematic of Bioreactor (Flow Configuration). The bioreactor consists of a rectangular Upper and Lower Chamber which contain nutrient media. Nutrient media recirculates through the upper chamber (length L of 4.57 cm, width b of 1.27 cm, height h of 350 μm) at a flow rate Q, applying a fluid-induced shear stress (τ) to the tissue, which resides on a semi-permeable membrane. Additional bioreactor details, including to-scale drawings, can be found in previous reports (Gemmiti and Guldberg 2006; Pierre et al. 2007).
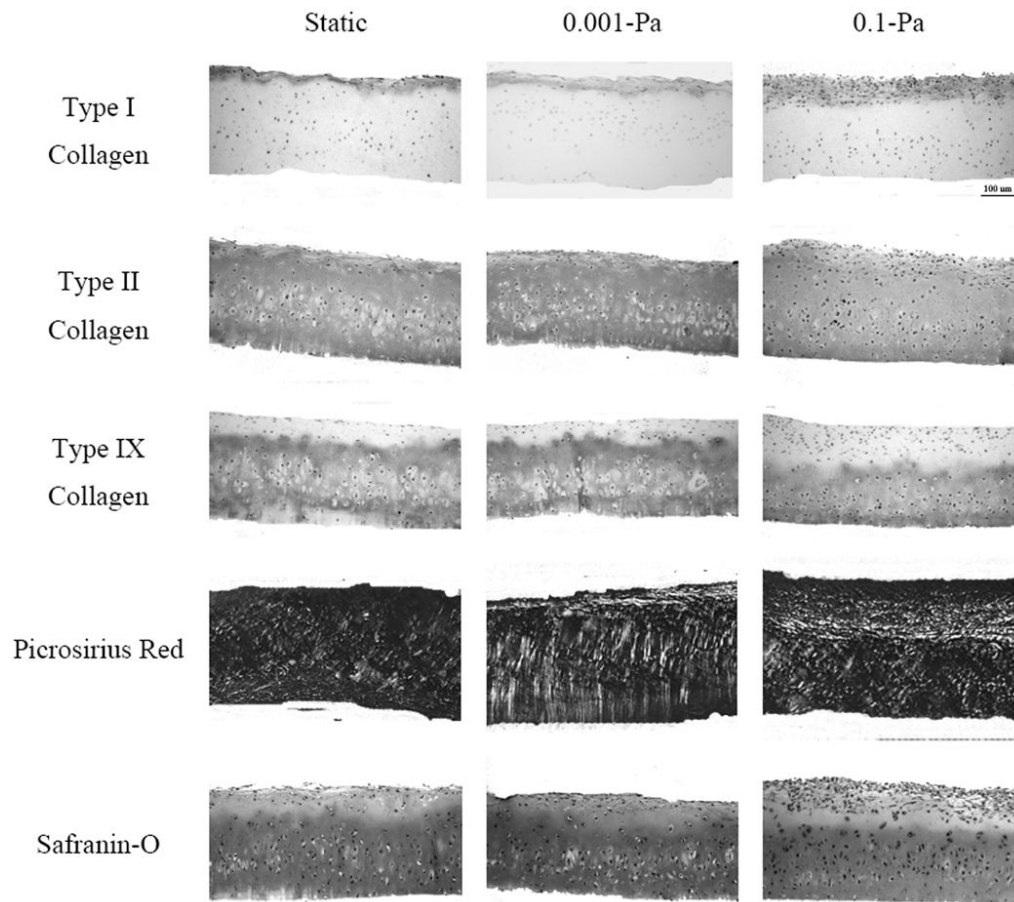
Figure 2.
Histology. Representative cross-sections for static, flow at 0.001-Pa and flow at 0.1-Pa when stained for type I, II, and IX collagen, total collagen (picrosirius red, birefringent light) and sulfated glycosaminoglycans (Safranin-O). Note the increase in type I collagen content co-localized with flattened, fibroblastic cells.
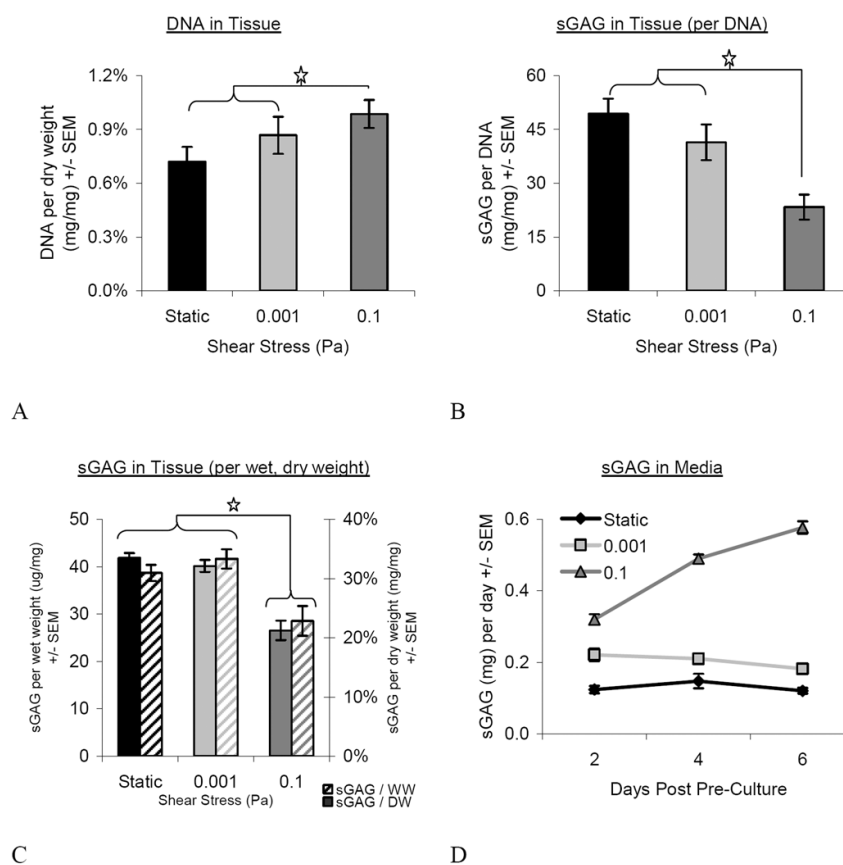
Figure 3.
Matrix Composition. Tissues flowed at 0.1-Pa possessed a greater number of cells (A), but less sGAG on a per-cell (B) and per-dry and per-wet weight (C) basis than the other groups. More sGAG was present in the media across all groups (D, significance not shown). However, no difference was found between groups when media and tissue contributions were summed (not shown). [N= 8-11 for A, B and C; N=4 per day for D] Star represents p≤0.05. Overall ANOVA values for the treatment of flow was p<0.0001 for all groups (A, total DNA; B, sGAG per-cell; C, sGAG per-weight).
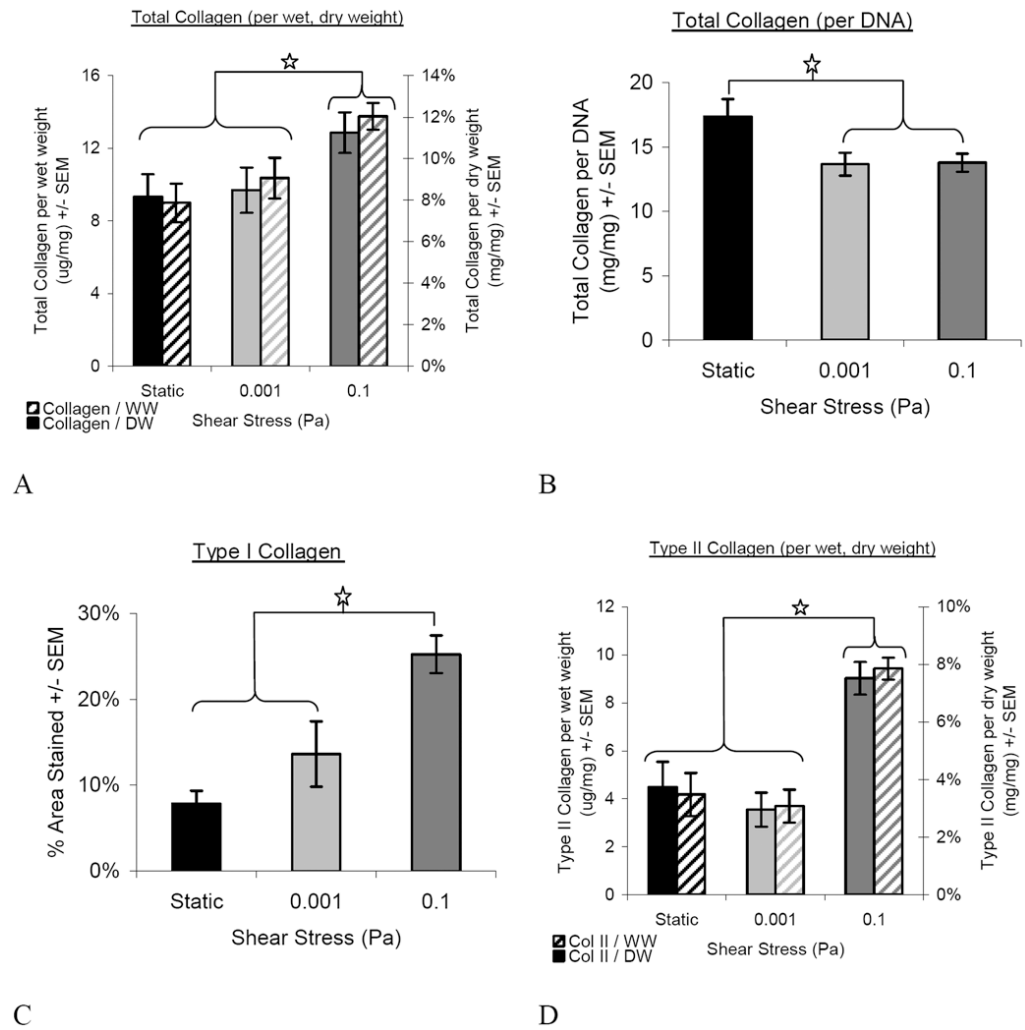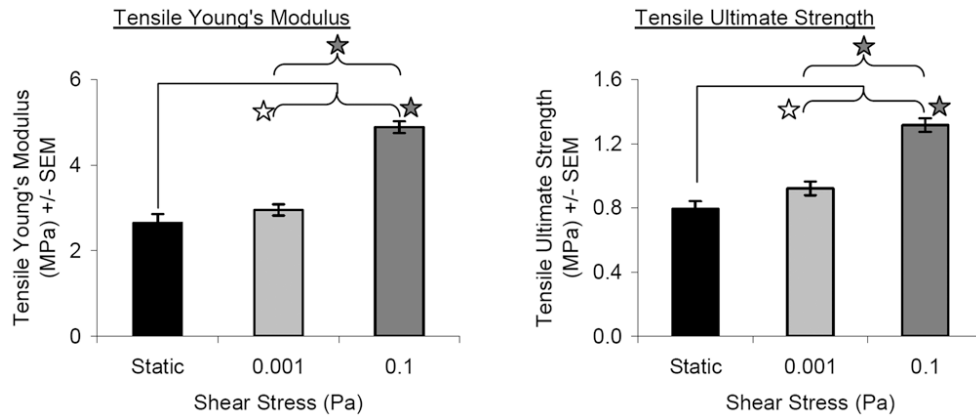
Figure 4.
Collagen Content. 0.1-Pa flow tissues contained more total collagen on a dry and wet weight basis (A) than the other groups, but the static group contained the most total collagen on per cell basis (B). The increase in total collagen was from contributions of both type I (C) and type II (wet and dry) (D) collagen; both types were significantly increased in 0.1-Pa flow compared to other groups. Star represents p≤0.05. Overall ANOVA values for the treatment of flow was p=0.012 (A, total collagen per-weight) and p<0.0001 (B, total collagen per-cell; C, type I collagen; D, type II collagen).

Figure 5.
Mechanical Properties. Both flow conditions resulted in higher Young's modulus (A) and ultimate strength (B) than the static condition. The higher flow group (0.1) was also significantly increased compared to the lower flow group (0.001). Shaded stars denote significance $p < 0.0001$ whereas open stars denote significance $p = 0.046$ for Young's modulus (A) and $p = 0.005$ for ultimate strength (B). Overall ANOVA values for the treatment of flow was $p < 0.0001$ for both Young's modulus and ultimate strength. [N=9-14] Star represents $p \leq 0.05$.
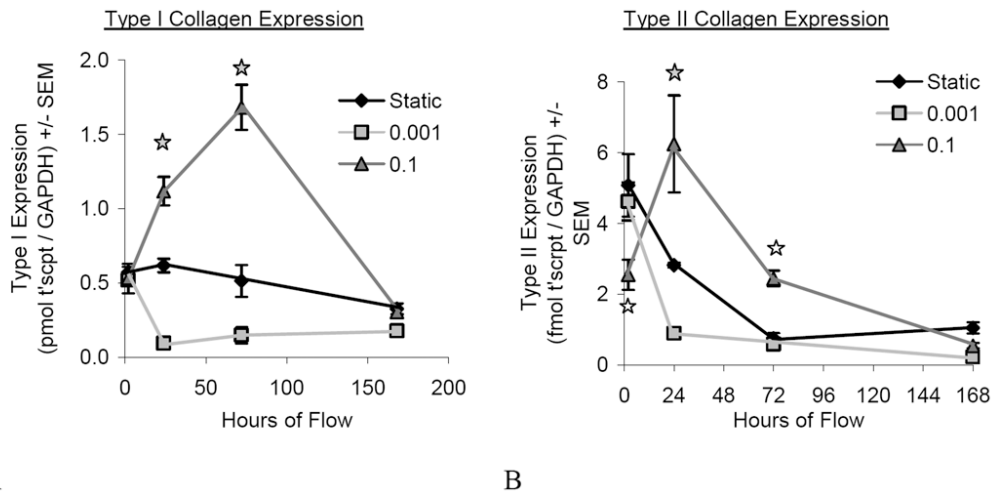
Figure 6.
Gene Expression. Type I (A) and type II (B) collagen are modulated by shear stress magnitude and duration of application, most notably at the 24- and 72-hour time points. Open stars denote significance ($p < 0.05$) for 0.1-Pa compare to other groups at that time point, whereas shaded stars represent significance ($p < 0.05$) between all groups at that time point. [N=3-4 for 2, 24, 72h; N=7-9 for 168h]

Table I

Primer sequences used for target genes in quantitative PCR reactions.

Target Gene (all bovine)	Primer Sequences (5′-3′)
Aggrecan	Forward: CCT CAG GGT TTC CTG ACA TTA Reverse: TAA GCT CAG TCA CGC CAG ATA
Type I Collagen (Hunter et al. 2002)	Forward: AAG AAC CCA GCT CGC ACA TG Reverse: GGT TAG GGT CAA TCC AGT AGT AAC CA
Type II Collagen (Hunter et al. 2002)	Forward: GCA TTG CCT ACC TGG ACG AA Reverse: CGT TGG AGC CCT GGA TGA
GAPDH	Forward: CCT TCA TTG ACC TTC ACT ACA TGG TCT A Reverse: TGG AAG ATG GTG ATG GCC TTT CCA TTG

Table II

Averages ± SEM for construct thickness, percentage water, wet and dry mass for each condition. There were no significant differences between groups.

Flow Condition	Thickness (μm)	% Water	Total Wet Mass (mg)	Total Dry Mass (mg)
Static	304.3 ± 2.7	88.5 ± 0.4%	274.9 ± 5.8	31.7 ± 1.2
0.001-Pa	304.3 ± 11.9	87.0 ± 0.6%	262.8 ± 7.8	34.3 ± 2.0
0.1-Pa	317.2 ± 8.1	86.7 ± 0.0%	272.1 ± 4.1	35.8 ± 2.1